Palaeogeography, Palaeoclimatology, Palaeoecology 567 (2021) 110242

Contents lists available at ScienceDirect

Palaeogeography, Palaeoclimatology, Palaeoecology

journal homepage: www.elsevier.com/locate/palaeo

Reconstructing early Holocene seasonal bottom-water temperatures in the northern North Sea using stable oxygen isotope records of *Arctica islandica* shells

Tamara Trofimova [a,*], Carin Andersson [a], Fabian G.W. Bonitz [a], Leif-Erik Rydland Pedersen [b], Bernd R. Schöne [c]

[a] NORCE Norwegian Research Centre, Bjerknes Centre for Climate Research, Jahnebakken 5, 5007 Bergen, Norway
[b] Department of Earth Science, University of Bergen, Allégaten 41, 5007 Bergen, Norway
[c] Institute of Geosciences, University of Mainz, Johann-Joachim-Becher-Weg 21, 55128 Mainz, Germany

ARTICLE INFO

Keywords:
Bivalves
Seasonality
Paleotemperature proxy
Reproducibility
Seasonal stratification dynamics

ABSTRACT

The knowledge of seasonal temperature variability in the ocean is essential for understanding climate and its response to forcing factors. Time intervals with highly dynamic climate and increased seasonal forcing such as the early Holocene are of particular interest. Yet, the temporal resolution of most existing climate records is not sufficient to reconstruct temperature seasonality. Here, we present the first seasonally resolved, early Holocene, bottom-water temperature record from the Viking Bank in the northern North Sea. The reconstruction is based on the stable oxygen isotope data ($\delta^{18}O_{shell}$) of two crossdated, radiocarbon-dated subfossil shells of *Arctica islandica* (Bivalvia). Oxygen isotope data were combined into a 21-year long record, dated at 9593–9573 (±55) cal yr BP The record indicates an early Holocene seasonal temperature amplitude up to ca. 4.5 °C. To estimate changes in the mean state and seasonality of temperature conditions between the present and early Holocene, the record and temperatures inferred thereof are compared with modern $\delta^{18}O_{shell}$ profiles and instrumental temperature data. The results indicate that the seasonal amplitude of $\delta^{18}O_{shell}$ signal in the subfossil shells reflects sea-level changes. The reconstruction suggests that the long-term average and seasonal variability of temperature were similar to modern times when considering changes in the relative sea level. Our data also confirm that $\delta^{18}O_{shell}$ records are reproducible and track seasonal amplitude of bottom-water temperature variability, thus demonstrate the potential for application in reconstructions of past seasonality. Furthermore, our results show that $\delta^{18}O_{shell}$ records can be used to reconstruct seasonal stratification dynamics. This novel application of sclerochronological data has the potential to be used to validate and constrain paleotidal models.

1. Introduction

The early Holocene (ca. 11,500–8000 cal yr BP) climate in the North Atlantic region was highly dynamic and characterized by abrupt climatic fluctuations (e.g., Mayewski et al., 2004; Bakke et al., 2005; Nesje et al., 2005; Hou et al., 2011). A prominent feature of early Holocene marine climate records in the northeastern subpolar North Atlantic is a distinct thermal maximum (Hald et al., 2007). As evidenced in sediment core records from the Barents Sea and Svalbard margin, this was the warmest interval within the entire Holocene (Hald et al., 2004, 2007; Ebbesen et al., 2007). The early Holocene thermal maximum is commonly associated with the Holocene summer insolation maximum in the Northern Hemisphere (Renssen et al., 2009, 2012), which occurred around 12,000–10,000 cal yr BP (Berger and Loutre, 1991) and is connected with an increase in seasonality.

Available marine records from the mid-latitudes do not show a consistent pattern of early Holocene warmth (e.g., Andersson et al., 2010 and references therein) and indicate temperature conditions as warm as, or slightly warmer than the present, depending on the proxy used (Birks and Koç, 2002; Calvo et al., 2002; Dolven et al., 2002; Risebrobakken et al., 2003; Andersen et al., 2004; Hald et al., 2007). The difference in trends between the southern and northern records was

* Corresponding author.
E-mail addresses: tatr@norceresearch.no (T. Trofimova), caan@norceresearch.no (C. Andersson), fabian.bonitz@hvl.no (F.G.W. Bonitz), leif-erik.pedersen@uib.no (L.-E.R. Pedersen), schoeneb@uni-mainz.de (B.R. Schöne).

https://doi.org/10.1016/j.palaeo.2021.110242
Received 4 June 2020; Received in revised form 6 January 2021; Accepted 7 January 2021
Available online 16 January 2021

suggested to be related to a polar amplification of early Holocene warmth linked to the seasonality of the orbital forcing (Hald et al., 2007). Risebrobakken et al. (2011) later showed that high-latitude radiative forcing might not be responsible for overall water column conditions, particularly the subsurface water temperatures. However, most marine paleoenvironmental reconstructions, including those mentioned above, are based on proxies, which typically represent an annual mean temperature or an average over the summer season. Furthermore, the temporal resolution of these records is not sufficient to reconstruct temperature seasonality. None of these records could provide a full picture of seasonality at the time. Yet, this information is essential for our understanding of climate and its response to different forcing factors. There are also indications that, during time intervals of rapid climatic fluctuations, summer and winter climate did not always change synchronously, and, for example, a decrease in annual mean temperature can be dominated by winter conditions (Denton et al., 2005). The important role of seasonality in explaining abrupt climate fluctuations (Denton et al., 2005) and the latitudinal contrast of early Holocene warmth (Renssen et al., 2012) demands a specific focus on inter-annual temperature variability in studies of early Holocene climate. There is a need for proxy records from key oceanographic localities that can provide information on early Holocene temperature seasonality and help to contextualize findings on the mean climate state based on proxies in sediment cores.

In this study, we examine the stable oxygen isotope composition of bivalve shells of *Arctica islandica*. Shells of this species provide means for high-resolution environmental reconstructions with solid temporal constraints (Scourse et al., 2006, Schöne, 2013). Like many other bivalve species, *A. islandica* builds its shell by incremental precipitation of calcium carbonate and forms annual growth increments delineated by growth lines. Shell carbonate of *A. islandica* precipitates near isotope equilibrium with ambient seawater with respect to oxygen (e.g., Weidman et al., 1994) and the fractionation is temperature-dependent. Previous studies using live-collected specimens demonstrated that $\delta^{18}O$ values of the shell could be used to faithfully reconstruct water temperatures at seasonal to annual time-scales (Weidman et al., 1994; Foster et al., 2009; Mette et al., 2016). Temperature reconstructions based on *A. islandica* shells are increasingly used to study the seasonality of the marine climate during time intervals in the more distant past (e.g., early Pleistocene) and the last millennium ((Buchardt and Símonarson, 2003) Schöne and Fiebig, 2009, Beierlein et al., 2015, Crippa et al., 2016, Von Leesen et al., 2017).

The focus of this study is on high-resolution $\delta^{18}O_{shell}$ records from the Viking Bank, northern North Sea (Fig. 1) and the potential of such records for studying early Holocene seasonality. Here, we present the first crossdated, seasonally resolved, early Holocene bottom-water temperature proxy record. The Viking Bank is an excellent locality for early Holocene marine environment reconstructions. Present-day hydrography of this area is controlled by the inflow of warm and saline Atlantic water from the easternmost branch of the North Atlantic Current – the Norwegian Atlantic current (NwAC) (Furnes et al., 1986; Orvik and Niiler, 2002). Foraminiferal records from the vicinity suggest a similar oceanographic regime was present during the early Holocene (Klitgaard-Kristensen et al., 2001). The heat transport of the NwAC plays an important role in the regional climate and is a principal component of the global climate system today, and has been throughout the entire Holocene (Risebrobakken et al., 2011; Eldevik et al., 2014).

To aid interpretation of the early Holocene climatic signal in the $\delta^{18}O_{shell}$ record, we examine the oxygen isotope signature of shells of live-collected *A. islandica* specimens from the study site. Modern seasonally resolved $\delta^{18}O_{shell}$ profiles were analyzed in the context of observational data to test the reliability of the $\delta^{18}O_{shell}$ records for seasonality reconstructions. For further assessment of the reproducibility and reliability of $\delta^{18}O_{shell}$-based temperature reconstructions, we compare temporally aligned geochemical profiles of specimens that lived during the same time interval, for both modern and early Holocene shells. By comparing the climatic signal in the $\delta^{18}O_{shell}$ records from modern and subfossil shells, we aim to estimate changes in the mean state and seasonality of temperature conditions between the present and the early Holocene.

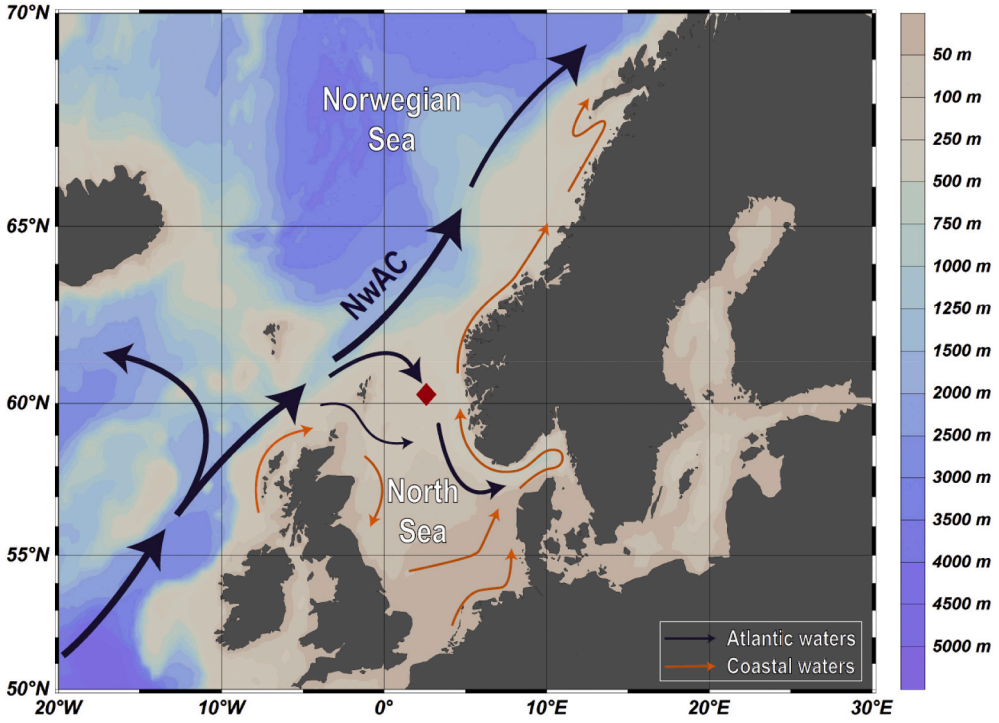

Fig. 1. Bathymetric map of the North Sea and the surrounding area showing sampling location, the circulation pattern of the Norwegian Atlantic Current (NwAC), and general surface circulation pattern in the North Sea, including the direction of the northern inflow of Atlantic water. The map was generated using Ocean Data View (http://odv.awi.de/).

2. Material and methods

2.1. Shell origin and preparation

Subfossil shells and living specimens of *A. islandica* were collected by bottom dredging at the Viking Bank in the northern North Sea (Fig. 1, Table 1) during a cruise on R/V *G.O. Sars* in November 2014. The specimens of *A. islandica* collected alive were frozen and later dissected onboard. From that material, four specimens were selected for subsequent analysis. Two specimens are well-preserved subfossil single valves (EH1, EH2), and another two specimens (M1, M2) were collected alive. The subfossil specimens were selected based on preservation status (Butler et al., 2020) and morphology, suggesting potential dating placement to the early Holocene. Relatively large, thick shells with no remaining periostracum are typical for the Viking Bank's early Holocene deposits (Andersson, unpublished data). The live-collected specimens were chosen based on ontogenetic age. Due to ontogenetic decline in the shell growth rate, the highest sampling resolution can only be archived in ontogenetically young shell portions (Schöne, 2013). To enable the construction of high-resolution oxygen isotope records representing the most recent decades, we selected shells of ontogenetically young specimens (<30 yr). All four selected specimens come from four close-by sampling sites (maximum distance between locations is ca. 12.5 km) and a water depth of 91 to 102 m (Table 1). One valve of each selected specimen was used for further investigation.

Selected valves were cut parallel to the axis of maximum growth and mounted on a glass slide with Buehler EpoxiCure 2 Resin. Using a low-speed high precision saw (IsoMet™, Buehler), 1–2 cm thick sections were cut along that axis. The sections attached to the glass slide were used for further sampling for stable isotope analysis. They were ground with the progressively finer grit size carbide paper (P1000, P2500, P4000), rinsed with demineralized water and air-dried. The 'mirroring' sections were embedded into epoxy blocks, ground with carbide paper, polished with diamond paste, and etched for 2 min in 0.1 M HCl. For the growth pattern analysis, acetate peel replicas of the etched surface were made (e.g., Thompson et al., 1980, Richardson, 2001).

2.2. Dating of shell material

Subfossil shells used in this study have been radiocarbon dated with Accelerator Mass Spectrometry (^{14}C AMS) at the Poznań Radiocarbon Laboratory in Poland. To prepare samples, the outermost shell surface, including adhering sediment particles, was mechanically removed using a handheld drill. Subsequently, chunks of carbonate samples (~40 mg) were cut from the ventral margin. Each sample represents the 10–15 most recent years of shell growth. The ^{14}C AMS dates (Table 1) suggest that the selected subfossil shells lived during overlapping time intervals.

To provide a temporal framework for constructing stable oxygen isotope records, we analyzed growth patterns of live-collected and subfossil shells. The acetate replicas were examined and photographed using a transmitted light microscope with 50× and 100× magnification. In such photographs, the annual growth lines were identified and counted to determine the ontogenetic age of the selected specimens (Table 1). In addition, annual growth increment widths (the distances between neighboring growth lines) were measured at the ventral shell margin, from the boundary between the outer and inner portions of the outer shell layer perpendicularly to the following growth line (e.g., Schöne, 2013). Based on similar relative changes in annual increment widths in specimens of the same group (live-collected or subfossil), increment width series were visually crossmatched (Fig. 2A, B; e.g., Butler et al., 2009, see also Black et al., 2019). Based on these results and the known date of death, each annual growth increment of live-collected shells was absolutely dated (i.e., exact calendar age assigned; 2A). For the subfossil shells, given the sufficient length of annual growth increment width series, visual crossmatching was statistically tested using SHELLCORR, run in Matlab (Fig. 3A,B; (Scourse et al., 2006). The results confirm the ^{14}C AMS dating and visual crossmatching, suggesting that the subfossil shells lived during the same time interval and began to form

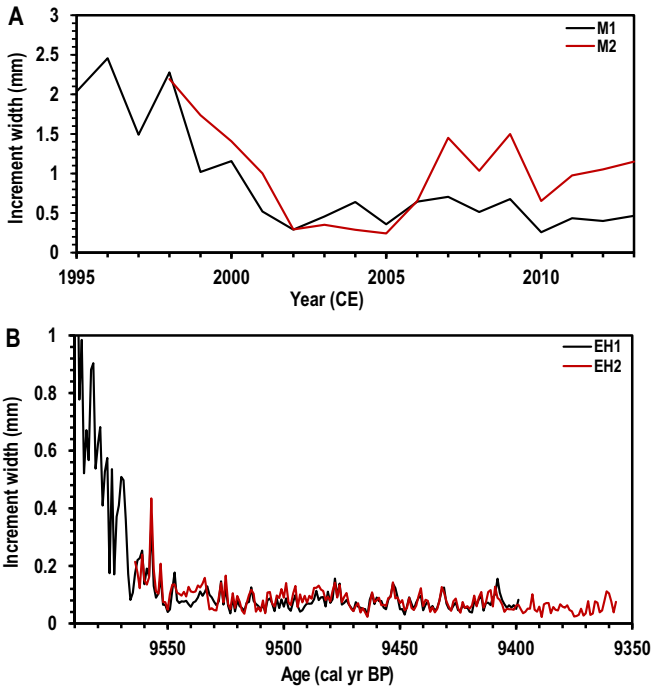

Fig. 2. Crossdated annual growth increment width series of (A) modern, live-collected shells and (B) subfossil specimens. Calendar ages assigned to individual growth increments by counting annual growth lines from the ventral margin to the umbo and taking into account the dating of the most recently formed increments based on (A) known date of collection (absolute dating, live-collected shells) and (B) calibrated ^{14}C AMS dates (± 55 cal yr BP; subfossil shells). Note: due to shell morphology, which limits the accuracy and consistency of increment width measurements at the ventral margin, ontogenetically young shell portions (2–6 years) were not measured. An interruption on the acetate peel of the shell EH2, although it did not obstruct visual crossmatching, further impeded uninterrupted measurements.

Table 1
List of specimens used in this study, including information on their ontogenetic ages and radiocarbon ages (^{14}C AMS and calibrated) of subfossil specimens.

Shell ID	Location of shell collection site	Depth of collection (m)	Ontogenetic age (yr)	Time interval	Lab ID	^{14}C AMS age (yr BP)	Calibrated age (cal yr BP ± 1σ)
EH1	60° 15′N 2° 10′E	99	197	Early Holocene	Poz-77543	8900 ± 35	9399 ± 55
EH2	60° 14′N 2° 11′E	102	233	Early Holocene	Poz-77503	8820 ± 50	9357 ± 55
M1	60° 13′N 2° 19′E	91	26	Modern	–	–	–
M2	60° 12′N 2° 17′E	95	17	Modern	–	–	–

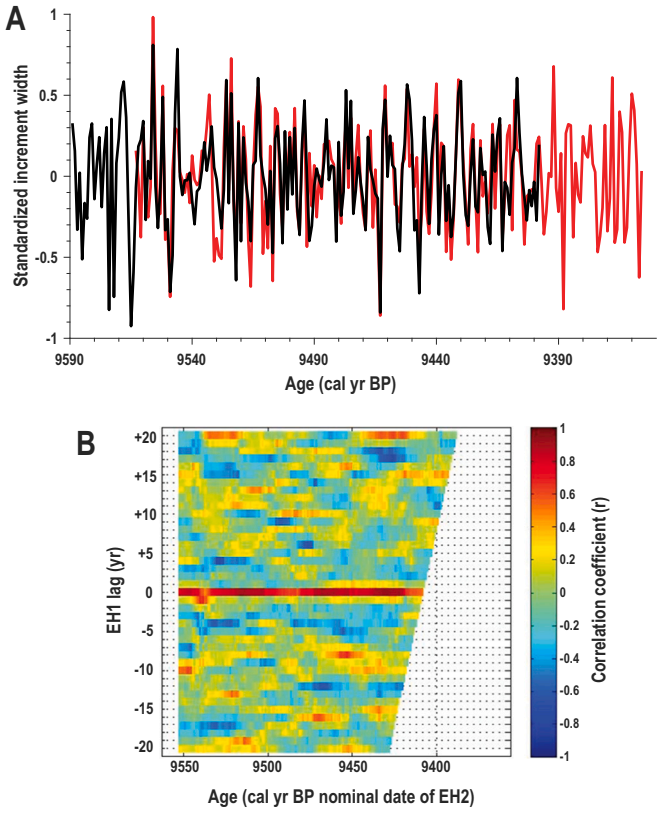

Fig. 3. (A) Crossdated, detrended, standardized growth increment width series of subfossil shells (EH1 in back, EH2 in red). The calendar ages were assigned to individual growth increments based on visual crossmatching and calibrated ^{14}C AMS dates (± 55 cal yr BP). To produce the plot, raw increment width series were logarithm-transformed, then the residuals from a 15-yr spline calculated and the resulted data were standardized. (B) The SHELLCORR graphical output showing lagged running correlations (window width 21 years) between EH1 and EH2 growth band series (for details see Scourse et al., 2006). High positive correlations are shown in red, high negative correlations in blue. Correlation between shells EH1 and EH2 shows the best continuous correlation at 0-yr lag, thus confirming the results of the visual crossmatching. (For interpretation of the references to colour in this figure legend, the reader is referred to the web version of this article.)

four years apart from each other.

Based on crossmatching, the relative position of radiocarbon-dated annual growth increments was determined. It allowed performing wiggle-matching of the radiocarbon dates to adjust the calibration based on crossmatching of individual growth increments (e.g., Helama and Hood, 2011). The calibration of the ^{14}C AMS dates, including wiggle-matching (Bronk Ramsey et al., 2001), was performed using OxCal v4.4 (Bronk Ramsey, 2009) and the MARINE20 calibration curve (Heaton et al., 2020) using a regional value for the marine reservoir correction (ΔR) of = −140 ± 35 years (^{14}CHRONO Marine Reservoir Database; www.calib.org), estimated based on measurements in bivalve shells from the Viking Bank (Mangerud and Gulliksen 1975).

2.3. Preservation of shell material

A good preservation status of the material is essential to use the shell oxygen isotope values for environmental reconstructions. Therefore, subfossil shells were visually examined for signs of diagenesis. The shell areas dedicated for stable isotope analysis were subsequently checked for recrystallization (from aragonite to calcite) with random single spot measurements (size 1–2 μm) using an 800 HR Raman spectrometer linked to an Olympus BX41 petrographic microscope (Raman laboratory at the Department of Earth Science, University of Bergen). The Raman spectra were acquired with a 514 nm Ar-ion laser with an absolute laser power of 15–20 mW. The laser went through a density filter (D = 0.3), 50× objective, and aperture hole with a diameter of 100 μm. Raman spectra were obtained in multiwindow mode with 5 s integration time and a spectral range of 100 to 1200 cm^{-1}. Obtained spectra were treated with the software Lab Spec version 5.58.25 and compared with previously published spectra of *A. islandica* shell aragonite (Milano et al., 2017).

No signs of diagenesis have been found based on visual examination, nor did the Raman spectra of the subfossil shells indicated traces of calcite. Therefore, studied shell portions were considered pristine aragonite and thus suitable for further geochemical analysis.

2.4. Stable oxygen isotope analysis and temperature reconstruction

Selected specimens were sampled for oxygen isotope analysis. Previously, it has been shown that sampling from different sub-layers in the outer shell layer can affect the oxygen isotope results in *A. islandica* shell carbonate (Trofimova et al., 2018). In this study, to ensure comparable results, the sampling was limited to the outer portion of the outer shell layer (oOSL). Before sampling, the periostracum and any surface contamination were removed by physically removing the outer ca. 10 μm of the outer shell surface. Shell carbonate samples were taken using an industrial high-precision drill (Minimo One Series, V. 2, Minitor Co., Ltd), attached to a binocular microscope, and equipped with a conical drill bit (300 μm diameter at the tip). Guided by the orientation of the growth lines, carbonate powder samples were produced by drilling consecutive and overlapping grooves in outer shell surface following the widely used serial sampling technique (e.g., Krantz et al., 1987; Mueller-Lupp et al., 2004; Purroy et al., 2018). All samples were extracted using a fixed drill speed of ca. 1000 rpm. The sampling was made in approximately the same ontogenetic years in all analyzed shells. Depending on the increment width, the sampling resolution ranges from 4 to 26 samples per year. Each sample yielded 40–120 μg of shell aragonite powder. To determine the reproducibility of the stable oxygen isotope signal between individuals and to assess the effect of the changes in sampling resolution on the seasonality range estimations, the sampling was performed in overlapping chronological intervals, as indicated by sclerochronological crossdating (Table 2).

Stable oxygen isotope measurements were conducted using a CF-IRMS Finnigan MAT 253 equipped with a Gas Bench II at the Institute of Geoscience at the University of Mainz, Germany. Carbonate samples were reacted with water-free phosphoric acid in He-flushed borosilicate exetainers at 72 °C. Stable oxygen isotope values are reported relative to the Vienna Pee-Dee Belemnite (VPDB) based on an NBS-19 calibrated internal lab standard (Carrara Marble; $\delta^{18}O = -1.91‰$). The long-term external precision (1σ), based on 421 blind analyses of NBS-19, was better than ±0.04‰, and the average internal precision based on eight injections per sample was better than 0.06‰. According to previous

Table 2
Sampling information.

Shell ID	Number of years sampled	Calendar years sampled (cal yr BP / yr CE)	Ontogenetic years sampled	Min - Max (average) sampling resolution (sample/year)	Total number of analyzed samples
EH1	15	9593–9579 (±55) BP	3–17	6–24 (9.3)	144
EH2	17	9589–9573 (±55) BP	3–19	4–26 (10)	175
M1	12	1990–2001 CE	3–14	6–12 (9.4)	117
M2	16	1997 –2013 CE	2–17	4–13 (9.5)	152

estimations based on annually resolved sampling (Trofimova et al., 2018), the reproducibility of homogenized shell aragonite powder samples is better than ±0.12‰. Note that we did not apply a correction for different acid fractionation factors of the shell samples (aragonite) and the reference material (calcite). For a more detailed explanation, see Füllenbach et al. (2015).

Considering the results of growth pattern analysis and sclerochronological crossdating, $\delta^{18}O_{shell}$ profiles were constructed. In such profiles, a sclerochronological year represents one growing season. Each sample within the isotope profile corresponds to a certain portion of the growing season, which is determined by the sampling resolution (number of samples per year) within a selected growth increment. Since the exact timing of the formation of each sampled shell portion is unknown, for ease of the analysis, in the resulting age model, all samples are assumed to represent an equal portion of time.

To compare the results of the stable oxygen isotope measurements and to test the reproducibility of the signal recorded in the shells, data of contemporaneous specimens have to be temporally aligned. This alignment was done individually for every year within the overlapping time intervals by visual wiggle-matching the seasonal isotope curves with AnalySeries 2.0.

The isotope values of the subfossil shells were corrected for the ice-volume effect by subtracting 0.28‰. This correction factor has been defined based on the work of Fairbanks (1989). By correcting for ice-volume effects, the early Holocene $\delta^{18}O_{shell}$ values that were obtained from the subfossil specimens are comparable to those of modern shells. Ice-volume corrected early Holocene $\delta^{18}O_{shell}$ values and modern shell oxygen isotope data were used to calculate the seasonal variability of the bottom-water temperature. Seawater temperatures were calculated using the paleotemperature equation (Eq. (1)) of Grossman, and Ku (1986) in the corrected version by Dettman et al. (1999):

$$T_{\delta 18O}\ (^{\circ}C) = 20.6–4.34 \times \left(\delta^{18}O_{shell} – \left(\delta^{18}O_{seawater} – 0.27\right)\right) \quad (1)$$

For the modern and early Holocene reconstructions, the $\delta^{18}O_{seawater}$ was assumed to be +0.37‰, based on previous estimates for the study area (Trofimova et al., 2018), which matches closely the $\delta^{18}O_{seawater}$ values recorded in the area close to our shell collection site (Harwood et al., 2008). The estimates by Trofimova et al. (2018) were obtained using the North Sea mixing line (Harwood et al., 2008), average salinity data (35.3 PSU; ICES database, www.ices.dk) and mean seasonal range of salinity changes (0.1 PSU; WOA 1° grid set, (Zweng et al., 2013). According to these estimates, the uncertainty related to typical seasonal changes in the salinity at the shell collection site equals ca. 0.03‰, which is less than the analytical precision of the stable isotope measurements, and therefore was neglected. Considering the reproducibility of homogenized shell aragonite powder samples (± 0.12‰ at 1σ; Trofimova et al., 2018), the estimated error of the reconstructed shell temperature estimates is ±0.5 °C.

2.5. Environmental data

To estimate the typical annual range of water temperature variability at the shell collection site, we used monthly means (data over three decades: 1985–1994, 1995–2004, and 2005–2012; grid cell 60.5°N 2.5°E.) extracted from the WOA 1° grid set (Locarnini et al., 2013; Zweng et al., 2013), available online (www.nodc.noaa.gov). The range was defined as the difference between the average temperature over three decades of the warmest and the coldest months at a target water depth. The observed temperature extremes (i.e., maximum and minimum recorded at a target water depth) were derived from CTD data sampled opportunistically with semi-monthly resolution (ICES oceanographic database, www.ices.dk) covering the measurements from 1990 to 2013 in the area 60-61°N and 2-3°E.

3. Results

3.1. Modern stable oxygen isotope profiles and reconstructed temperatures

The $\delta^{18}O_{shell}$ values measured in the live-collected specimens of *A. islandica* vary within a range of 2.08–3.19‰ (Fig. 4A; Supplementary Material 1), which translates into a temperature range between 11.9 and 7.2 °C. The oxygen isotope profiles derived from these specimens do not show clear seasonal cycles. However, growth lines (indicating the end of a growing season; Fig. 4A) are typically associated with a decrease of $\delta^{18}O_{shell}$ values and followed by a $\delta^{18}O_{shell}$ increase in the first samples after the growth line (seen in the direction of growth). The reconstructed seasonality range, i.e., the difference between annual maximum and minimum $\delta^{18}O_{shell}$ values, varies between 0.13 and 0.84‰, which corresponds to a seasonal temperature amplitude of 0.6 to 3.7 °C. The maximum $\delta^{18}O_{shell}$ significantly correlates with the sampling resolution ($r = 0.49$; $p = 0.02$), while no significant correlation was found between the minimum $\delta^{18}O_{shell}$ and sampling resolution.

A comparison of the stable oxygen isotope profiles of two specimens within the 5-year overlapping interval shows a generally good agreement between the data (Fig. 4A). During this time interval, the annual average $\delta^{18}O_{shell}$ values are within the limits of the analytical precision of the measurements (<0.07‰). The difference between the annual minima is less than 0.1‰, while the annual maxima $\delta^{18}O_{shell}$ values differ, on average, by 0.18‰. However, in one year (1999), the difference between the maximum $\delta^{18}O_{shell}$ values is as high as 0.40‰ (Fig. 4A).

3.2. Early Holocene stable oxygen isotope profiles and reconstructed temperatures

The ice-volume corrected early Holocene $\delta^{18}O_{shell}$ values vary between 1.75 and 3.28‰ (Fig. 4B; Supplementary Material 2), which corresponds to reconstructed temperatures of 13.4 to 6.8 °C, respectively. The profiles show distinct seasonal cycles, which are most pronounced within the first 10–15 ontogenetic years (increments sampled with >7 samples per year). Similar to the observations in the modern shells, the most positive $\delta^{18}O_{shell}$ values in each increment occur within the first samples in each increment (Fig. 4B). The reconstructed seasonality range varies between 0.29 and 1.06‰, which translates into an annual temperature range of 1.3 to 4.6 °C.

Within the 11-year overlapping time interval between early Holocene stable oxygen isotope profiles, the average difference between the annual mean $\delta^{18}O_{shell}$ values (in years without a hiatus in the data) is 0.14 ± 0.09‰. However, in one year (year 9580; Fig. 4B), the values are offset by 0.53‰. The annual minimum and maximum values of the compared years differ, on average, by 0.18‰ and 0.21‰, respectively.

4. Discussion

Proxy-based reconstructions are always an approximation of actual environmental conditions. An assessment of the reproducibility and reliability of proxy data for environmental reconstructions are important steps that should precede the interpretation of a proxy signal. Although the oxygen isotope data of *A. islandica* shells are considered to serve as a reliable proxy for water temperature (Schöne, 2013), the reproducibility of shell-derived isotope records often remains challenging (e.g., Mette et al., 2018; Trofimova et al., 2018). Moreover, there are indications that in some areas, shell-based reconstructions might overestimate actual water temperatures (e.g., Bonitz et al., 2018). Therefore, the reproducibility of $\delta^{18}O_{shell}$ records from different populations and their reliability for reconstructing water temperature require further testing. Here, we will address these aspects and then interpret early Holocene $\delta^{18}O_{shell}$ data in terms of paleotemperature seasonality.

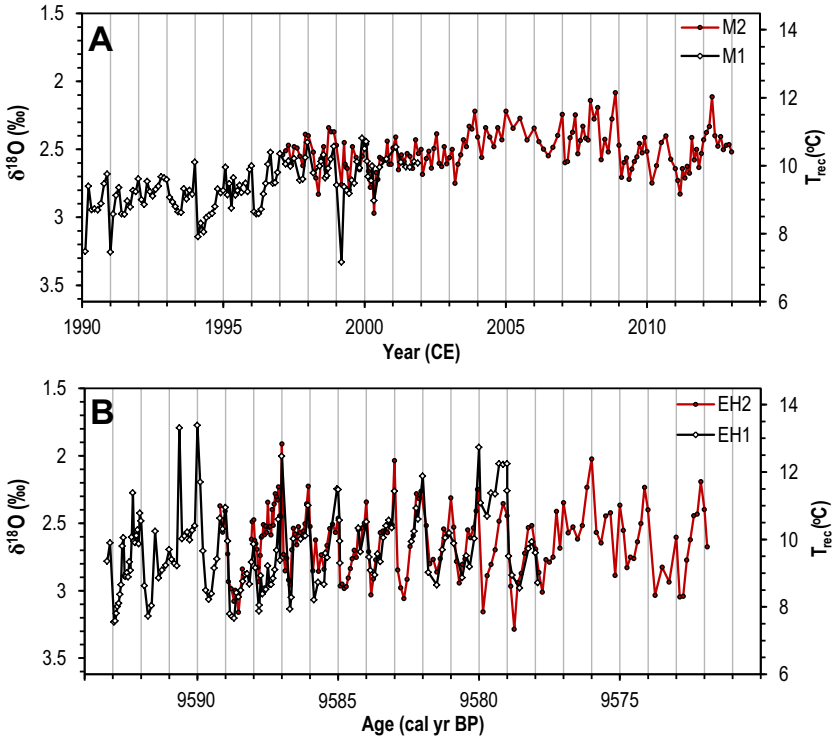

Fig. 4. Temporally aligned stable oxygen isotope ($\delta^{18}O_{shell}$ ‰ VPDB) profiles and reconstructed temperatures ($T^{o}_{rec}C$) of modern (A) and early Holocene (B) specimens. Calendar ages assigned based on sclerochronological crossdating and (A) known date of collection (absolute dating, live-collected shells) and (B) calibrated ^{14}C AMS dates (± 55 cal yr BP; subfossil shells). The grey vertical lines correspond to the position of the annual growth lines and indicate the end of the growing season (sclerochronological year). Note, breaks in the line connecting the values indicate missing samples.

4.1. *Reproducibility of the oxygen isotope signal*

The sclerochronological approach (i.e., crossdating) used in this study enables temporal alignment of the geochemical profiles of specimens that lived during the same time interval. It provides a unique opportunity to assess the reproducibility of the stable oxygen isotope signal. The comparison of temporally aligned stable oxygen isotope profiles within overlapping time intervals generally shows a good agreement in both live-collected and subfossil shell records (Fig. 4). In line with previous studies on the reproducibility of $\delta^{18}O_{shell}$ records in bivalves (e.g., Gillikin et al., 2005; Elliot et al., 2003), the differences observed between isotope profiles can mainly be explained by the spatiotemporal resolution of sampling. A low sampling resolution results in greater time-averaging within each sample and brings the seasonal amplitude closer to an annual mean (Goodwin et al., 2003). The greater time-averaging explains the smaller reconstructed range in $\delta^{18}O_{shell}$ in annual growth increments sampled with lower resolution (i.e., < 7 samples per increment), as well as the less pronounced seasonal cycle observed in the ontogenetically older portions of subfossil shells (Fig. 4B). Furthermore, sampling by drilling can result in an underrepresentation of parts of the growing season, and seasonal extremes can appear attenuated. This, for example, can explain the difference of ca. 0.28‰ between the seasonal $\delta^{18}O_{shell}$ minimum in the year 9586 (±55 cal yr BP) and ca. 0.41‰ in the year 9579 (±55 cal yr BP) of the early Holocene specimens (Fig. 4B) as well as the ca. 0.4‰ difference in year the 1999 CE in the live-collected specimens (Fig. 4A).

In a few instances, however, the deviations between $\delta^{18}O_{shell}$ profiles cannot just be explained by differences in sampling resolution, e.g., the offsets in the year 9588 (±55 cal yr BP) and 9580 (±55 cal yr BP) in the early Holocene record (Fig. 4B). Although in the year 9588 (±55 cal yr BP), the inter-specimen difference between seasonal extremes is negligible (0.05 and 0.09‰, respectively), profiles are offset, on average, by ca. 0.23‰, which translates into a temperature difference of ca. 1.0 °C. In the year 9580 (±55 cal yr BP), the offset is even larger, i.e., up to ca. 0.53‰ (= ca. 2.3 °C). The reason for these offsets is unclear considering the good agreement in other years. These deviations may potentially indicate a difference in local environmental conditions; respective shells were collected at a distance of ca. 9 km from each other. Nonetheless, other factors, including unknown methodological issues that might have occurred during sampling extraction and curation, cannot be excluded. Due to the poor reproducibility apparent from the significant offset between the seasonality estimates for the year 9580 (±55 cal yr BP), these data were omitted from further analysis.

The deviations between isotope profiles in the overlapping years imply that the results can be biased if the analyses are limited to a single specimen. However, on average, the difference between the annual mean $\delta^{18}O_{shell}$ values is only 0.03 ± 0.02‰ for live-collected specimens and 0.14 ± 0.09‰ for the early Holocene specimens. These results are close to or smaller than the observations in other bivalve records (e.g., 0.19‰ in *Saxidomus gigantea* (Gillikin et al., 2005); 0.25–0.76‰ in *Tridacna derasa*, (Yamanashi et al., 2016)), and smaller than the average between-colony $\delta^{18}O$ variability recorded in corals (0.20–0.40‰) (e.g., Linsley et al., 1999; Guilderson and Schrag, 1999). The overall good agreement between the data shows that the $\delta^{18}O_{shell}$ can be reproduced in both modern and subfossil shell material. Hence, the recorded signal is environmentally controlled and reliable climate records can be generated from $\delta^{18}O_{shell}$ profiles. Moreover, the agreement between subfossil oxygen isotope profiles supports the crossdating and demonstrates the high potential for constructing longer (> 30 years), high-resolution floating records reflecting past seasonality. The use of chronologies as the temporal framework for high-resolution sampling provides an opportunity to include multiple specimens in the same record. This permits a reduction in the sampling resolution limits associated with the ontogenetic decline in shell growth rate. An analysis of long high-resolution $\delta^{18}O_{shell}$ records enables us to study the long-term variability in the seasonal cycle and, thus, the stability of the seasonality through time.

4.2. Modern $\delta^{18}O_{shell}$ records and seasonality estimates in the northern North Sea

The analysis of modern $\delta^{18}O_{shell}$ records in the context of present climate conditions is crucial for assessing the reliability of shell-based seasonality reconstructions and the evaluation of potential limitations of the method. The stable oxygen isotope composition of shell carbonate is a function of both the biomineralization temperature and the isotope composition of ambient seawater. However, the oxygen isotope signal can be modulated by factors related to the life history of the animals (e.g., duration and timing of the growing season) and oceanographic conditions of the habitat (e.g., water depth, circulation patterns). To interpret $\delta^{18}O_{shell}$ profiles as records of seasonality, the role of these factors should be carefully evaluated.

One of the important aspects for interpretation of $\delta^{18}O_{shell}$ signals is the water depth in which the animals lived, as it affects the annual mean and the range of seasonal variations in water temperature. There are indications that the shape of the $\delta^{18}O_{shell}$ curves can provide clues on the depth of the habitat relative to the thermocline (Schöne and Fiebig, 2009). The $\delta^{18}O_{shell}$ curves derived from the shells of *A. islandica,* which lived above a seasonal thermocline, in waters vertically mixed throughout the year are nearly sinusoidal (skewed sinusoidal) with relatively large seasonal swings (Schöne et al., 2004; Schöne et al., 2005a; Schöne et al., 2005b; Foster et al., 2009; Bonitz et al., 2018). In settings below the thermocline, seasonal temperature variability is lower (Austin et al., 2006) and the $\delta^{18}O_{shell}$ curves are typically saw-tooth shaped with a lack of clear seasonal cycle and low seasonal amplitudes (Schöne and Fiebig, 2009; Schöne et al., 2005b). Regardless of the locality and habitat of mollusks, annual growth lines are typically associated with low $\delta^{18}O_{shell}$ values, followed by a $\delta^{18}O_{shell}$ increase, which is consistent with our observations. In the present study, oxygen isotope profiles derived from live-collected shells do not show distinct sinusoidal cycles, but a saw-tooth shaped pattern (Fig. 4A). This indicates a small range of temperature variability throughout the growing season, which is typical for a habitat below the thermocline and supported by observational data. In the study area, the water column is thermally stratified during summer, with the lower limit of the thermocline at 20–50 m (Lee, 1980) and low seasonal variability of temperature and salinity at the bottom (ca. 2.1 °C and ca. 0.1 PSU, respectively).

The seasonal range, as reflected in $\delta^{18}O_{shell}$ profiles, depends on the duration and timing of the growing season of the mollusks. Studies on live-collected specimens demonstrate that the timing of the growing season varies between populations, but primarily depends on the depth of the habitat relative to the thermocline (Schöne, 2013). Based on previously published data, irrespective of the population, the length of the main growing season usually exceeds seven months (Schöne et al., 2004; Ballesta-Artero et al., 2017; Jones, 1980; Weidman et al., 1994). Previous findings and our observations (small seasonal range in $\delta^{18}O_{shell}$) suggest that a sampling resolution of fewer than seven samples per increment may not be sufficient to reconstruct the full seasonal range. Therefore, $\delta^{18}O_{shell}$ data representing increments sampled with lower resolution were not used for reconstructing the seasonal temperature ranges.

The seasonal ranges inferred from $\delta^{18}O_{shell}$ values in live-collected specimens vary between 0.8 and 3.7 °C, and are, on average, ca. 1.7 °C. These estimates are in agreement with observations from the study location. However, the reconstructed temperature amplitude is slightly smaller. According to the observational data, the average range between the warmest and the coldest months is ca. 2.1 °C, while the range between minimum and maximum observed temperatures since 1990 is 4.5 °C. Since the seasonal maximum in $\delta^{18}O_{shell}$ is significantly correlated with the sampling resolution, the truncated seasonality of the shell-derived temperatures could be explained by a decrease in the shell growth rate occurring during the cold months, which has also previously been suggested for the populations from the northern North Sea (Witbaard et al., 2003), including our shell collection site (Trofimova et al., 2018). According to Witbaard et al. (2003), shell growth in these populations is reduced during spring due to the limited food supply (e.g. Davies and Payne, 1984), which is in agreement with the more recent studies on the factors triggering *A. islandica* shell growth (Ballesta-Artero et al., 2017, 2018). The reduced growth rate during spring suggests that the annual temperature maxima are very likely to be recorded in the isotope profiles, while the annual minima may not be. However, studies of populations of *A. islandica* inhabiting shallower (< 50 m) parts of the North Sea showed that shell growth is not limited to the warmest part of the year and that the temperature minima can be faithfully reconstructed from the $\delta^{18}O_{shell}$ data (Schöne et al., 2005a; Schöne et al., 2005b). Hence, the decrease in the shell growth during cold months and associated limitations for reconstructing the full seasonal temperature range may only be specific to deeper water habitats.

The verification of the shell-based reconstructions requires comparison with observational data. However, the potential for making comparisons at our sampling locality is limited by the lack of high-resolution instrumental data with sufficient spatial coverage. Furthermore, the lack of a distinct seasonal cycle in the $\delta^{18}O_{shell}$ data further complicates the comparison with the limited observational data, making the verification impossible. To check how well shell-based reconstructions represent the seasonal temperature conditions in the study area, we compared the results with the typical annual temperature range, and the minimum and maximum temperatures as given by available CTD data (Fig. 5). This comparison shows that the average reconstructed range is offset from observations by ca. 1.0 °C. The reason for this offset is unclear but could be related to a difference in the time-averaging between the observational and proxy data, deviation from expected oxygen isotope fractionation, and/or a different $\delta^{18}O_{water}$ value than assumed.

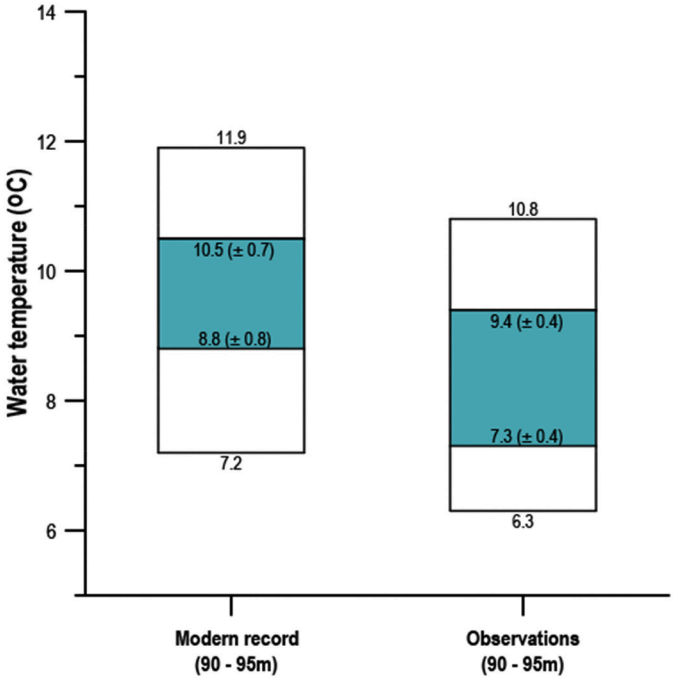

Fig. 5. Observed and reconstructed seasonal temperature amplitude based on live-collected shells in the study area. The observational data are represented by the average temperature of the warmest and coldest month (shown by the upper and lower limits of the inner box) and the maximum and minimum water temperatures given by CTD data since 1990 (upper and lower limits of the outer box). The amplitude of the reconstructed temperatures is defined as the average maximum and minimum reconstructed water temperatures based on the annual growth increments sampled with a resolution of ≥7 samples per year (shown by the upper and lower limits of the inner box). The outer box shows the range of absolute extreme water temperatures of the shell-based reconstructions.

Furthermore, previous studies have shown that the sampling techniques (e.g., milling setup; Waite and Swart, 2015) and strategy (e.g., target shell layer; Trofimova et al., 2018), as well as the sample curation methods (e.g., Tobin et al., 2011), can alter isotope results from biogenic aragonite, hence affect reconstructed temperature values. The study on shells of *A. islandica* from the Faroe shelf (Bonitz et al., 2018) using a technique similar to the one in the present study, report a similar offset between reconstructed temperatures and observations, suggesting that the sampling-related issues can lead to an overestimation of reconstructed temperatures. Regardless of the reason, our results indicate that shell-based reconstructions can be used to faithfully estimate relative changes in the water temperature. However, it is possible that the reconstructed range in our data is overestimated by ~1 °C.

4.3. Early Holocene seasonality in $\delta^{18}O_{shell}$ records

The comparison of isotope signal in early Holocene record with its modern analog and other proxy data facilitates a better understanding of the past climate conditions and their relative changes through time. Proxy evidence from the study area suggests that the early Holocene oceanography in the northern North Sea was controlled by the inflow of Atlantic water (Peacock, 1995) and characterized by bottom-water temperature conditions similar to present (Klitgaard-Kristensen et al., 2001; Hald et al., 2007). In our study, however, oxygen isotope records of subfossil shells indicate environmental conditions different from those recorded in the modern oxygen isotope profiles. In contrast to oxygen isotope profiles derived from live-collected shells, the early Holocene record displayed distinct seasonal cycles (Fig. 4). Oxygen isotope profiles exhibited a skewed sinusoidal pattern, similar to that observed in modern shells of bivalves from the North Sea living above the thermocline (Schöne and Fiebig, 2009). A comparison of the $\delta^{18}O_{shell}$ data obtained with identical sampling resolution indicates that the seasonal amplitude in the early Holocene record is significantly higher than in modern shells (paired *t*-test, $p \leq 0.01$). The early Holocene $\delta^{18}O_{shell}$ record is characterized by lower seasonal minima and higher seasonal maxima (Fig. 4). The shape of the isotope curves and the larger seasonal $\delta^{18}O_{shell}$ amplitudes argue for a shallower habitat with a water column vertically mixed throughout the year.

The generally lower global sea level during the early Holocene compared to today (Smith et al., 2011) can explain our findings. According to lithological and macrofaunal data from the study area, before the beginning of the Holocene (14,000–16,000 cal yr BP), the Viking Bank was dry land (Peacock, 1995). Since then, relative sea level had continuously risen to 80–100 m below the present level at 12,000 cal yr BP. During the early Holocene, the sea level continued to rise rapidly and, as suggested by Peacock (1995), after 12,000 cal yr BP, the glacio-isostatic sea-level changes in the Viking Bank area were similar to those associated with the Barbados glacio-eustatic sea-level curve (Fairbanks, 1989). This would imply a water depth at the shell collection site of ca. 45–50 m at ~9600 cal yr BP. Existing paleogeographic model results provide similar or slightly higher estimates (≥ 50 m) for the local paleowater depth at this time (Shennan et al., 2000, Lambeck, 1995, Sturt et al., 2013, Harff et al., 2017). These results indicate that the water depth was half of what it is today, which explains the seasonal $\delta^{18}O_{shell}$ signal in the early Holocene record. The shallower depth and associated changes in tidal dynamics could have hindered the development of a seasonal thermocline, which implies that the water column at the shell collection site was tidally mixed throughout major parts of the year. This interpretation is supported by the paleotidal simulations predicting a transition of the water column from a tidally mixed to a stratified state at the study site, at a timing roughly coinciding with our shell record (Uehara et al., 2006; Ward et al., 2016).

The depth of the habitat can affect the extent of the growing season, thus controlling the seasonality range reconstructed from the shells. A previous study on mollusks from the North Sea living at a shallower depth today (ca. 50 m; Schöne et al., 2005b) suggests that the extent of the growing season allows us to reconstruct the full seasonal temperature cycle. Considering these findings, it is likely that the early Holocene $\delta^{18}O_{shell}$ records from the Viking Bank can be used to reconstruct the full seasonal temperature range. In contrast, this is likely cannot be accomplished with shells of modern bivalves from the same locality.

Sub-annual $\delta^{18}O_{seawater}$ variations associated with salinity changes affect the range of seasonality recorded in $\delta^{18}O_{shell}$ profiles (e.g., Schöne, 2013). Large fluctuations in salinity can obscure temperature signal by decreasing the expected seasonal amplitude of $\delta^{18}O_{shell}$ variability in the record. Although the local salinity and its seasonal variability during early Holocene have not been determined, large salinity changes compared to the relatively stable present-day conditions, cannot explain a higher $\delta^{18}O_{shell}$ seasonality range in our paleorecord. Nevertheless, without independent estimates of salinity and its changes on a sub-annual scale, we cannot exclude that the seasonal temperature range was somewhat larger than the reconstructed range. However, the remote location from potential freshwater sources and the control of oceanographic conditions by Atlantic water inflow (Klitgaard-Kristensen et al., 2001) argue against highly variable salinity conditions on a seasonal scale. Therefore, we assume that the stable oxygen isotope signal in the early Holocene records is controlled mainly by the seasonal temperature variability rather than changes in the isotope composition of seawater. The difference between isotope signals in modern and early Holocene records, thus, primarily reflects changes in relative sea level and associated variability in local stratification dynamics. This suggests that the $\delta^{18}O_{shell}$ records can be used to reconstruct the seasonal thermocline development, thus providing empirical data needed to validate and constrain paleotidal models (Ward et al., 2020).

Taking into account the paleowater depth estimates, the amplitude of the seasonal water temperature reconstructed from subfossil shell oxygen isotope data can be compared with modern observational data

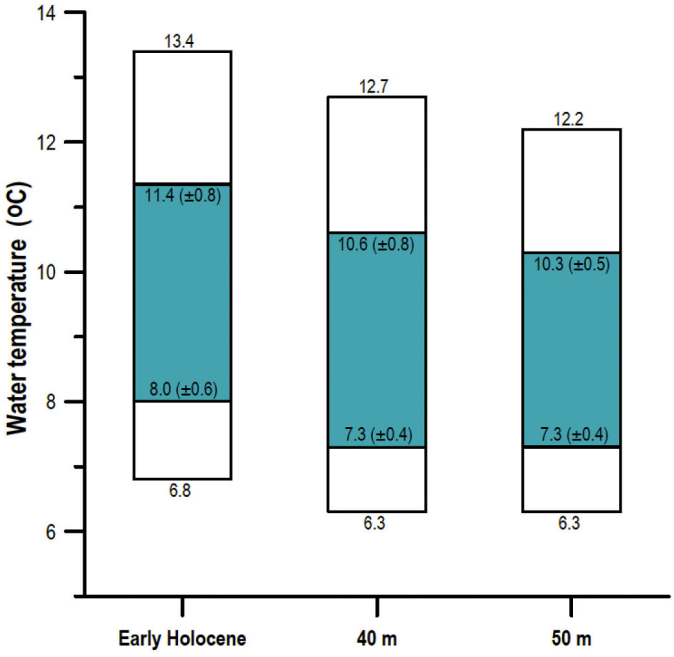

Fig. 6. Average observed and reconstructed water temperature amplitudes. The observational data for the depth 40 and 50 m represented by the average temperature of the warmest and coldest month (shown by the upper and lower limits of the inner boxes) and the maximum and minimum water temperatures given by CTD data since 1990 (upper and lower limits of the outer box). The amplitude of the reconstructed temperatures is defined as the average maximum and minimum reconstructed water temperature at a resolution of ≥7 samples per year (shown by the upper and lower limits of the inner box). The limits of the outer box show the absolute minimum and maximum water temperatures given by the shell-based reconstructions.

from the Viking Bank. This comparison shows that the average range closely matches the range observed at a depth of 40 to 50 m (Fig. 6), which is in line with paleowater depths estimates for the shell collection site (45-50 m). Considering a possible offset of ca. 1 °C in computed temperatures, as suggested by isotope data of live-collected shells, the absolute values of the interannual temperature variability are also in agreement (within error) with those observed today. According to the observational data, the average annual temperature at a depth of 45 m is around 8.7 °C, which is in agreement with the average temperature inferred from the early Holocene record (8.5 ± 0.6 °C, corrected for the offset). The similarity in range and average temperatures suggest a seasonality regime similar to modern conditions.

To check how well reconstructed early Holocene sub-annual temperature variability corresponds to modern conditions, the records were placed in the seasonal temporal context, considering paleowater depth estimates (ca. 45 m). This was done by aligning the reconstructed seasonal temperature extremes (the data corrected for the offset of ca. 1.0 °C) with those in the instrumental data from the target water depth (45 m) so that the temperatures of the subfossil isotope data fitted to the shape of modern temperature curve (Fig. 7). The results show that the reconstructed early Holocene seasonality corresponds well to the modern seasonal cycle. Following the alignment of the isotope curves, the main growing season of the early Holocene shells was likely between January and October. However, in some years, the growing season might have been more extended, and after a short cessation, shell growth resumed as early as in November. The timing and length of the estimated growing season of early Holocene specimens correspond well with observations on modern populations in the North Sea. Above the thermocline, the shell growth is reduced or halted between September and November, while in the deeper settings, a shell growth reduction occurs between December and February (Schöne, 2013). In both cases, the shell growth slows down after the warmest temperatures have been attained, which is in agreement with our interpretation of the data.

The reconstructed seasonal temperature cycle is associated with an error related to the uncertainties in paleowater depth estimates, absolute $\delta^{18}O_{seawater}$ values, and their seasonal and inter-annual variability, as well as the above-mentioned methodological issues. Nevertheless, our results suggest average temperature conditions similar to the present, which correspond well with previous reconstructions of the mean

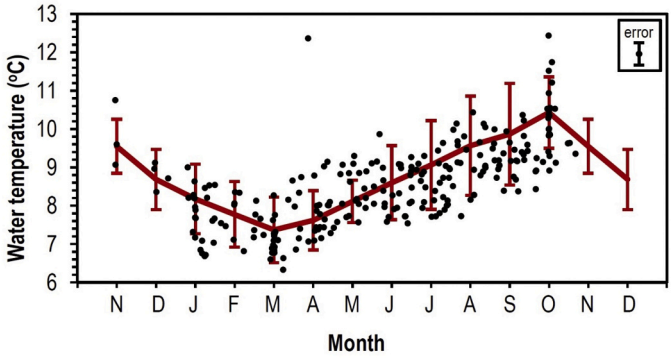

Fig. 7. The reconstructed early Holocene seasonal bottom-water temperatures (black dots) and modern water temperatures at a depth of 45 m (red line; data from WOA 1° grid set (Locarnini et al., 2013)). The temperature reconstruction is based on oxygen isotope data of 17 calendar years and a sampling resolution exceeding seven samples per year. The error bar in the inlay depicts the analytical uncertainty of the reconstructed seasonal bottom-water temperatures based on the sample reproducibility and accuracy of the mass spectrometer (Trofimova et al., 2018). The modern seasonal water temperature cycle is represented by monthly means over three decades (1985–1994, 1995–2004, 2005–2012). The error bars indicate the standard deviation of the mean. (For interpretation of the references to colour in this figure legend, the reader is referred to the web version of this article.)

temperature conditions during the early Holocene based on foraminiferal records from the vicinity to our study site (Klitgaard-Kristensen et al., 2001; Hald et al., 2007). Our results also provide new insight on early Holocene seasonality, indicating that the inter-annual temperature cycle was similar to modern times. This similarity suggests that early Holocene higher-than present solar radiative forcing did not cause seasonal warming, thus might not have had a significant impact on the subsurface temperature conditions in the northern North Sea. This is in line with the previous study (Risebrobakken et al., 2011) based on a comparison of proxy-based temperature reconstructions and model results, concluding that "high radiative forcing is not responsible for the overall water column condition."

4.4. *Bivalve records of early Holocene seasonality and marine climate in the North Atlantic*

Presently, *A. islandica* commonly occurs on the continental shelves of the North Atlantic (Nicol, 1951). The early Holocene biogeographical distribution of this species may have been even wider, reaching Svalbard and the Arctic coast of Russia (Dahlgren et al., 2000; Zatsepin and Filatova, 1961). Nevertheless, the $\delta^{18}O_{shell}$ records of early Holocene are rare.

Previously, the oxygen isotope composition of *A. islandica* shells has been used to reconstruct the early Holocene (9954–9782 cal yr BP) seasonal bottom-water temperature regime at ca. 30 m depth in northern North Atlantic (Beierlein et al., 2015). By working with shell records from the Dicksonfjord (Svalbard), Beierlein et al. (2015) suggested that the seasonality was 50% stronger and average temperatures about 6 °C higher than today in the Svalbard area. These temperature estimates match previous estimates of the mean temperature condition based on sediment-core proxies (Hald et al., 2004; Ebbesen et al., 2007; Rasmussen et al., 2014). Similar estimates have been obtained based on the analysis of the geographical distribution of thermophilous mollusks (including *A. islandica*) in early Holocene deposits around Svalbard (Mangerud and Svendsen, 2017). The findings of Mangerud and Svendsen (2017), also indicate that the peak of the thermal maximum occurred between 10,200–9200 cal yr BP, which is consistent with a maximum of the ocean water heat transport by NwAC, as previously suggested by Risebrobakken et al. (2011).

The record presented here is dated at 9593–9573 (± 55) cal yr BP and thus coincides with the thermal maximum evidenced by the bivalve records from Svalbard, and possibly a few centuries younger than the *A. islandica* records from the Dicksonfjord. Due to the difference in timing and the initial oceanographic regime (different depth and water masses), the records are not comparable. However, it is possible to compare the relative difference between the reconstructed temperature regime and present-day observations at these localities. The significantly higher seawater temperatures and seasonality range off the coast of Svalbard (Beierlein et al., 2015) and the absence of a significant warming in the northern North Sea indicated by the results of the present study suggest a possible polar amplification of early Holocene warmth. Although any conclusions based on the comparison of only two very distant shell records must be treated with caution, this interpretation is consistent with the previous paleoclimatic reconstructions (e.g., Hald et al., 2007). The comparison of proxy data from sediment cores along S—N transect on the Norwedian-Svalbard continental margin (60°N to 70.4°N), suggest a smaller meridional temperature gradient and a significant polar amplification of the early Holocene warming (e.g., Hald et al., 2007). The similarity between reconstructions based on sediment-core proxies and bivalve sclerochronological records supports the validity of the findings.

5. Conclusions

The present study demonstrates that $\delta^{18}O_{shell}$ profiles of *A. islandica* from the northern North Sea can be used to generate reliable seasonal

temperature records for multiple decades at a time. The $\delta^{18}O_{shell}$ can be reproduced in both modern and subfossil shell material. However, particular care should be taken during sampling and interpretation of $\delta^{18}O_{shell}$ data. Methodological issues, such as the effect of the sampling resolution (preventing reconstruction of the actual temperature range) as well as the potential effect of sampling by milling on the $\delta^{18}O_{shell}$, have to be addressed before interpreting the data. Moreover, uncertainties related to the timing and duration of the growing season, collection depth, and inter-annual salinity (and hence $\delta^{18}O_{seawater}$) changes have to be taken into account to reconstruct past climatic conditions.

We have presented a 21-yr long crossdated shell-derived oxygen isotope record reflecting early Holocene temperature seasonality in the northern North Sea. Early Holocene $\delta^{18}O_{shell}$ profiles exhibit distinct seasonal patterns and an intra-annual range of up to 1.1‰, which converts into a temperature range of ca. 4.5 °C. The estimation of the mean temperature conditions is consistent with previous findings based on temperature proxies in sediment cores, which supports the reliability of shell-based reconstructions. Furthermore, our data provide unprecedented evidence that seasonal bottom-water temperatures in the northern North Sea during the early Holocene were likely similar to present-day conditions, and thus providing valuable knowledge for future studies of this time interval. The apparent contrast between the $\delta^{18}O_{shell}$ signal of modern and subfossil shells observed here reflect relative sea-level changes and associated variations in local tidal dynamics between the early Holocene and the present. According to our data, during the early Holocene (9593–9573 (±55) cal yr BP), the water column was vertically mixed throughout most parts of the year contrary to modern seasonally stratified conditions at the Viking Bank. Thus, our results demonstrate a novel application of sclerochronological data to reconstruct seasonal stratification dynamics.

Declaration of Competing Interest

The authors declare that they have no known competing financial interests or personal relationships that could have appeared to influence the work reported in this paper.

Acknowledgments

The authors thank Trygve Knag at the Department of Earth Science, University of Bergen, for the help regarding the analysis with Raman spectroscopy in this study. Further, the authors acknowledge help with the collection of the shell material provided by the crew of the R/V *G.O. Sars* and the ITN ARAMACC team. Financially support was given by the EU Framework Programme 7 (FP7), as part of the Marie Curie Initial Training Network ARAMACC (60482) and the Meltzer Research Fund. The authors also thank James Scourse and an anonymous reviewer and for thoughtful comments, which significantly improved the manuscript.

Appendix A. Supplementary data

Supplementary data to this article can be found online at https://doi.org/10.1016/j.palaeo.2021.110242.

References

Andersen, C., Koc, N., Jennings, A., Andrews, J.T., 2004. Nonuniform response of the major surface currents in the Nordic Seas to insolation forcing: implications for the Holocene climate variability. Paleoceanography 19. https://doi.org/10.1029/2002PA000873.

Andersson, C., Pausata, F.S.R., Jansen, E., Risebrobakken, B., Telford, R.J., 2010. Holocene trends in the foraminifer record from the Norwegian Sea and the North Atlantic Ocean. Clim. Past 6, 179–193. https://doi.org/10.5194/cp-6-179-2010.

Austin, W.E.N., Cage, A.G., Scourse, J.D., 2006. Mid-latitude shelf seas: a NW European perspective on the seasonal dynamics of temperature, salinity and oxygen isotopes. The Holocene 16, 937–947. https://doi.org/10.1177/0959683606hl985rp.

Bakke, J., Dahl, S.O., Nesje, A., 2005. Lateglacial and early Holocene palaeoclimatic reconstruction based on glacier fluctuations and equilibrium-line altitudes at northern Folgefonna, Hardanger, western Norway. J. Quat. Sci. 20, 179–198. https://doi.org/10.1002/jqs.893.

Ballesta-Artero, I., Witbaard, R., Carroll, M.L., van der Meer, J., 2017. Environmental factors regulating gaping activity of the bivalve *Arctica islandica* in Northern Norway. Mar. Biol. 164, 116. https://doi.org/10.1007/s00227-017-3144-7.

Ballesta-Artero, I., Janssen, R., van der Meer, J., Witbaard, R., 2018. Interactive effects of temperature and food availability on the growth of *Arctica islandica* (Bivalvia) juveniles. Mar. Environ. Res. 133, 67–77. https://doi.org/10.1016/j.marenvres.2017.12.004.

Beierlein, L., Salvigsen, O., Schone, B.R., Mackensen, A., Brey, T., 2015. The seasonal water temperature cycle in the Arctic Dicksonfjord (Svalbard) during the Holocene climate Optimum derived from sub-fossil *Arctica islandica* shells. The Holocene 25, 1197–1207. https://doi.org/10.1177/0959683615580861.

Berger, A., Loutre, M.-F., 1991. Insolation values for the climate of the last 10 million years. Quat. Sci. Rev. 10, 297–317. https://doi.org/10.1016/0277-3791(91)90033-Q.

Birks, C.J.A., Koç, N., 2002. A high-resolution diatom record of late-Quaternary Sea-surface temperatures and oceanographic conditions from the eastern Norwegian Sea. Boreas 31, 323–344. https://doi.org/10.1111/j.1502-3885.2002.tb01077.x.

Black, B.A., Andersson, C., Butler, P.G., Carroll, M.L., Delong, K.L., Reynolds, D.J., Schöne, B.R., Scourse, J., van der Sleen, P., Wanamaker, A.D., Witbaard, R., 2019. The revolution of crossdating in marine palaeoecology and palaeoclimatology. Biol. Lett. 15, 20180665. https://doi.org/10.1098/rsbl.2018.0665.

Bonitz, F.G.W., Andersson, C., Trofimova, T., Hátún, H., 2018. Links between phytoplankton dynamics and shell growth of *Arctica islandica* on the Faroe Shelf. J. Mar. Syst. 179, 72–87. https://doi.org/10.1016/j.jmarsys.2017.11.005.

Bronk Ramsey, C., 2009. Bayesian analysis of radiocarbon dates. Radiocarbon 51, 337–360. https://doi.org/10.1017/S0033822200033865.

Bronk Ramsey, C., Van Der Plicht, J., Weninger, B., 2001. 'Wiggle matching' radiocarbon dates. Radiocarbon 43, 381–389. https://doi.org/10.1017/S0033822200038248.

Butler, P.G., Richardson, C.A., Scourse, J.D., Witbaard, R., Schone, B.R., Fraser, N.M., Wanamaker, A.D., Bryant, C.L., Harris, I., Robertson, I., 2009. Accurate increment identification and the spatial extent of the common signal in five *Arctica islandica* chronologies from the Fladen Ground, northern North Sea. Paleoceanography 24, PA2210. https://doi.org/10.1029/2008PA001715.

Buchardt, B., Símonarson, L.A., 2003. Isotope palaeotemperatures from the Tjörnes beds in Iceland: evidence of Pliocene cooling. Palaeogeogr. Palaeoclimatol. Palaeoecol. 189, 71–95. https://doi.org/10.1016/S0031-0182(02)00594-1.

Butler, P.G., Fraser, N.M., Scourse, J.D., Richardson, C.A., Bryant, C., Heinemeier, J., 2020. Is there a reliable taphonomic clock in the temperate North Atlantic? An example from a North Sea population of the mollusc *Arctica islandica*. Palaeogeogr. Palaeoclimatol. Palaeoecol. 109975 https://doi.org/10.1016/j.palaeo.2020.109975.

Calvo, E., Grimalt, J., Jansen, E., 2002. High resolution U^{K}_{37} Sea surface temperature reconstruction in the Norwegian Sea during the Holocene. Quat. Sci. Rev. 21, 1385–1394. https://doi.org/10.1016/S0277-3791(01)00096-8.

Crippa, G., Angiolini, L., Bottini, C., Erba, E., Felletti, F., Frigerio, C., Hennissen, J.A.I., Leng, M.J., Petrizzo, M.R., Raffi, I., Raineri, G., Stephenson, M.H., 2016. Seasonality fluctuations recorded in fossil bivalves during the early Pleistocene: Implications for climate change. Palaeogeogr. Palaeoclimatol. Palaeoecol. 446, 234–251. https://doi.org/10.1016/j.palaeo.2016.01.029.

Dahlgren, T.G., Weinberg, J.R., Halanych, K.M., 2000. Phylogeography of the ocean quahog (*Arctica islandica*): influences of paleoclimate on genetic diversity and species range. Mar. Biol. 137, 487–495. https://doi.org/10.1007/s002270000342.

Davies, J.M., Payne, R., 1984. Supply of organic matter to the sediment in the northern North Sea during a spring phytoplankton bloom. Mar. Biol. 78, 315–324. https://doi.org/10.1007/bf00393017.

Denton, G.H., Alley, R.B., Comer, G.C., Broecker, W.S., 2005. The role of seasonality in abrupt climate change. Quat. Sci. Rev. 24, 1159–1182. https://doi.org/10.1016/j.quascirev.2004.12.002.

Dettman, D.L., Reische, A.K., Lohmann, K.C., 1999. Controls on the stable isotope composition of seasonal growth bands in aragonitic fresh-water bivalves (unionidae). Geochim. Cosmochim. Acta 63, 1049–1057. https://doi.org/10.1016/S0016-7037(99)00020-4.

Dolven, J.K., Cortese, G., Bjørklund, K.R., 2002. A high-resolution radiolarian-derived paleotemperature record for the late Pleistocene-Holocene in the Norwegian Sea. Paleoceanography 17, 1072. https://doi.org/10.1029/2002PA000780.

Ebbesen, H., Hald, M., Eplet, T.H., 2007. Lateglacial and early Holocene climatic oscillations on the western Svalbard margin, European Arctic. Quat. Sci. Rev. 26, 1999–2011. https://doi.org/10.1016/j.quascirev.2006.07.020.

Eldevik, T., Risebrobakken, B., Bjune, A.E., Andersson, C., Birks, H.J.B., Dokken, T.M., Drange, H., Glessmer, M.S., Li, C., Nilsen, J.E.Ø., Otterå, O.H., Richter, K., Skagseth, Ø., 2014. A brief history of climate – the northern seas from the last Glacial Maximum to global warming. Quat. Sci. Rev. 106, 225–246. https://doi.org/10.1016/j.quascirev.2014.06.028.

Elliot, M., Demenocal, P.B., Linsley, B.K., Howe, S.S., 2003. Environmental controls on the stable isotopic composition of *Mercenaria mercenaria*: potential application to paleoenvironmental studies. Geochem. Geophys. Geosyst. 4 https://doi.org/10.1029/2002GC000425.

Fairbanks, R.G., 1989. A 17,000-year glacio-eustatic sea level record: influence of glacial melting rates on the Younger Dryas event and deep-ocean circulation. Nature 342, 637–642. https://doi.org/10.1038/342637a0.

Foster, L.C., Allison, N., Finch, A.A., Andersson, C., Ninnemann, U.S., 2009. Controls on $\delta^{18}O$ and $\delta^{13}C$ profiles within the aragonite bivalve *Arctica islandica*. The Holocene 19, 549–558. https://doi.org/10.1177/0959683609104028.

Füllenbach, C.S., Schöne, B.R., Mertz-Kraus, R., 2015. Strontium/lithium ratio in aragonitic shells of *Cerastoderma edule* (Bivalvia) — A new potential temperature proxy for brackish environments. Chem. Geol. 417, 341–355. https://doi.org/10.1016/j.chemgeo.2015.10.030.

Furnes, G.K., Hackett, B., Sætre, R., 1986. Retroflection of Atlantic water in the Norwegian trench. Deep Sea Res. Part A Oceanogr. Res. Pap. 33, 247–265. https://doi.org/10.1016/0198-0149(86)90121-4.

Gillikin, D.P., De Ridder, F., Ulens, H., Elskens, M., Keppens, E., Baeyens, W., Dehairs, F., 2005. Assessing the reproducibility and reliability of estuarine bivalve shells (*Saxidomus giganteus*) for sea surface temperature reconstruction: Implications for paleoclimate studies. Palaeogeogr. Palaeoclimatol. Palaeoecol. 228, 70–85. https://doi.org/10.1016/j.palaeo.2005.03.047.

Goodwin, D.H., Schöne, B.R., Dettman, D.L., 2003. Resolution and fidelity of oxygen isotopes as paleotemperature proxies in bivalve mollusk shells: models and observations. PALAIOS 18, 110–125. https://doi.org/10.1669/0883-1351(2003)18<110:RAFOOI>2.0.CO;2.

Grossman, E.L., Ku, T.-L., 1986. Oxygen and carbon isotope fractionation in biogenic aragonite: Temperature effects. Chem. Geol. 59, 59–74. https://doi.org/10.1016/0168-9622(86)90057-6.

Guilderson, T.P., Schrag, D.P., 1999. Reliability of coral isotope records from the Western Pacific warm Pool: A comparison using age-optimized records. Paleoceanography 14, 457–464. https://doi.org/10.1029/1999PA900024.

Hald, M., Ebbesen, H., Forwick, M., Godtliebsen, F., Khomenko, L., Korsun, S., Ringstad Olsen, L. & Vorren, T. O., 2004. Holocene paleoceanography and glacial history of the West Spitsbergen area, Euro-Arctic margin. Quat. Sci. Rev. 23, 2075–2088. https://doi.org/10.1016/j.quascirev.2004.08.006.

Hald, M., Andersson, C., Ebbesen, H., Jansen, E., Klitgaard-Kristensen, D., Risebrobakken, B., Salomonsen, G.R., Sarnthein, M., Sejrup, H.P., Telford, R.J., 2007. Variations in temperature and extent of Atlantic Water in the northern North Atlantic during the Holocene. Quat. Sci. Rev. 26, 3423–3440. https://doi.org/10.1016/j.quascirev.2007.10.005.

Harff, J., Flemming, N.C., Groh, A., Hünicke, B., Lericolais, G., Meschede, M., Rosentau, A., Sakellariou, D., Uścinowicz, S., Zhang, W., Zorita, E., 2017. Sea Level and Climate. *Submerged Landscapes of the European Continental Shelf*. John Wiley & Sons, Ltd.

Harwood, A.J.P., Dennis, P.F., Marca, A.D., Pilling, G.M., Millner, R.S., 2008. The oxygen isotope composition of water masses within the North Sea. Estuar. Coast. Shelf Sci. 78, 353–359. https://doi.org/10.1016/j.ecss.2007.12.010.

Heaton, T.J., Köhler, P., Butzin, M., Bard, E., Reimer, R.W., Austin, W.E.N., Bronk Ramsey, C., Grootes, P.M., Hughen, K.A., Kromer, B., Reimer, P.J., Adkins, J., Burke, A., Cook, M.S., Olsen, J., Skinner, L.C., 2020. Marine20—the Marine Radiocarbon Age Calibration Curve (0–55,000 cal BP). Radiocarbon 62, 779–820. https://doi.org/10.1017/RDC.2020.68.

Helama, S., Hood, B.C., 2011. Stone Age midden deposition assessed by bivalve sclerochronology and radiocarbon wiggle-matching of *Arctica islandica* shell increments. J. Archaeol. Sci. 38, 452–460. https://doi.org/10.1016/j.jas.2010.09.029.

Hou, J., Huang, Y., Shuman, B.N., Oswald, W.W., Foster, D.R., 2011. Abrupt cooling repeatedly punctuated early-Holocene climate in eastern North America. The Holocene 22, 525–529. https://doi.org/10.1177/0959683611427329.

Jones, D.S., 1980. Annual cycle of shell growth increment formation in two continental shelf bivalves and its paleoecologic significance. Paleobiology 6, 331–340. https://doi.org/10.2307/2400349.

Klitgaard-Kristensen, D., Sejrup, H.P., Haflidason, H., 2001. The last 18 kyr fluctuations in Norwegian sea surface conditions and implications for the magnitude of climatic change: evidence from the North Sea. Paleoceanography 16, 455–467. https://doi.org/10.1029/1999PA000495.

Krantz, D.E., Williams, D.F., Jones, D.S., 1987. Ecological and paleoenvironmental information using stable isotope profiles from living and fossil molluscs. Palaeogeogr. Palaeoclimatol. Palaeoecol. 58, 249–266. https://doi.org/10.1016/0031-0182(87)90064-2.

Lambeck, K., 1995. Late Devensian and Holocene shorelines of the British Isles and North Sea from models of glacio-hydro-isostatic rebound. J. Geol. Soc. 152, 437–448. https://doi.org/10.1144/gsjgs.152.3.0437.

Lee, A.J., 1980. North Sea: physical oceanography. Elsevier Oceanogr. Ser. 24, 467–493.

Linsley, B.K., Messier, R.G., Dunbar, R.B., 1999. Assessing between-colony oxygen isotope variability in the coral *Porites lobata* at Clipperton Atoll. Coral Reefs 18, 13–27. https://doi.org/10.1007/s003380050148.

Locarnini, R.A., Mishonov, A.V., Antonov, J.I., Boyer, T.P., Garcia, H.E., Baranova, O.K., Zweng, M.M., Paver, C.R., Reagan, J.R., Johnson, D.R., Hamilton, M., Seidov, D., 2013. World Ocean Atlas 2013, volume 1: temperature. In: Levitus, S., Mishonov, A. (Eds.), NOAA Atlas NESDIS 73. NOAA, Silver Spring.

Mangerud, J., Gulliksen, S., 1975. Apparent radiocarbon ages of recent marine shells from Norway, Spitsbergen, and Arctic Canada. Quaternary Research 5, 263–273. https://doi.org/10.1016/0033-5894(75)90028-9.

Mangerud, J., Svendsen, J.I., 2017. The Holocene thermal maximum around Svalbard, Arctic North Atlantic; molluscs show early and exceptional warmth. The Holocene. https://doi.org/10.1177/0959683617715701.

Mayewski, P.A., Rohling, E.E., Stager, J.C., Karlén, W., Maasch, K.A., Meeker, L.D., Meyerson, E.A., Gasse, F., VAN Kreveld, S., Holmgren, K., 2004. Holocene climate variability. Quat. Res. 62, 243–255. https://doi.org/10.1016/j.yqres.2004.07.001.

Mette, M.J., Wanamaker, A.D., Carroll, M.L., Ambrose, W.G., Retelle, M.J., 2016. Linking large-scale climate variability with *Arctica islandica* shell growth and geochemistry in northern Norway. Limnol. Oceanogr. 61, 748–764. https://doi.org/10.1002/lno.10252.

Mette, M.J., Whitney, N.M., Ballew, J., Wanamaker, A.D., 2018. Unexpected isotopic variability in biogenic aragonite: A user issue or proxy problem? Chem. Geol. 483, 286–294. https://doi.org/10.1016/j.chemgeo.2018.02.027.

Milano, S., Nehrke, G., Wanamaker, A.D., Ballesta-Artero, I., Brey, T., Schöne, B.R., 2017. The effects of environment on *Arctica islandica* shell formation and architecture. Biogeosciences 14, 1577–1591. https://doi.org/10.5194/bg-14-1577-2017.

Mueller-Lupp, T., Bauch, H.A., Erlenkeuser, H., 2004. Holocene hydrographical changes of the eastern Laptev Sea (Siberian Arctic) recorded in $\delta^{18}O$ profiles of bivalve shells. Quat. Res. 61, 32–41. https://doi.org/10.1016/j.yqres.2003.09.003.

Nesje, A., Jansen, E., Birks, H.J.B., Bjune, A.E., Bakke, J., Andersson, C., Dahl, S.O., Kristensen, D.K., Lauritzen, S.E., Lie, Ø., 2005. Holocene climate variability in the northern North Atlantic region: a review of terrestrial and marine evidence. In: Drange, H., Dokken, T.M., Furevik, T., Gerdes, R., Berger, W.H. (Eds.), The Nordic Seas: An Integrated Perspective.

Nicol, D., 1951. Recent species of the veneroid pelecypod *Arctica*. J. Wash. Acad. Sci. 41, 102–106.

Orvik, K.A., Niiler, P., 2002. Major pathways of Atlantic water in the northern North Atlantic and Nordic Seas toward Arctic. Geophys. Res. Lett. 29, 1896. https://doi.org/10.1029/2002GL015002.

Peacock, J.D., 1995. Late Devensian to early holocene palaeoenvironmental changes in the Viking Bank area, northern North Sea. Quat. Sci. Rev. 14, 1029–1042. https://doi.org/10.1016/0277-3791(95)00041-0.

Purroy, A., Milano, S., Schöne, B.R., Thébault, J., Peharda, M., 2018. Drivers of shell growth of the bivalve, *Callista chione* (L. 1758) – combined environmental and biological factors. Mar. Environ. Res. 134, 138–149. https://doi.org/10.1016/j.marenvres.2018.01.011.

Rasmussen, T.L., Thomsen, E., Skirbekk, K., Ślubowska-Woldengen, M., Klitgaard Kristensen, D., Koç, N., 2014. Spatial and temporal distribution of Holocene temperature maxima in the northern Nordic seas: interplay of Atlantic-, Arctic- and polar water masses. Quat. Sci. Rev. 92, 280–291. https://doi.org/10.1016/j.quascirev.2013.10.034.

Renssen, H., Seppa, H., Heiri, O., Roche, D.M., Goosse, H., Fichefet, T., 2009. The spatial and temporal complexity of the Holocene thermal maximum. Nat. Geosci. 2, 411–414. https://doi.org/10.1038/ngeo513.

Renssen, H., Seppä, H., Crosta, X., Goosse, H., Roche, D.M., 2012. Global characterization of the Holocene thermal Maximum. Quat. Sci. Rev. 48, 7–19. https://doi.org/10.1016/j.quascirev.2012.05.022.

Richardson, C.A., 2001. Molluscs as archives of environmental change. Oceanogr. Mar. Biol. Annu. Rev. 39, 103–164.

Risebrobakken, B., Jansen, E., Andersson, C., Mjelde, E., Hevrøy, K., 2003. A high-resolution study of Holocene paleoclimatic and paleoceanographic changes in the Nordic Seas. Paleoceanography 18. https://doi.org/10.1029/2002PA000764.

Risebrobakken, B., Dokken, T.M., Smedsrud, L.H., Andersson, C., Jansen, E., Moros, M., Ivanova, E.V., 2011. Early Holocene temperature variability in the Nordic Seas: the role of oceanic heat advection versus changes in orbital forcing. Paleoceanography 26. https://doi.org/10.1029/2011PA002117.

Schöne, B.R., 2013. *Arctica islandica* (Bivalvia): A unique paleoenvironmental archive of the northern North Atlantic Ocean. Glob. Planet. Chang. 111, 199–225. https://doi.org/10.1016/j.gloplacha.2013.09.013.

Schöne, B.R., Fiebig, J., 2009. Seasonality in the North Sea during the Allerød and late medieval climate Optimum using bivalve sclerochronology. Int. J. Earth Sci. 98, 83–98. https://doi.org/10.1007/s00531-008-0363-7.

Schöne, B.R., Castro, A.D.F., Fiebig, J., Houk, S.D., Oschmann, W., Kroncke, I., 2004. Sea surface water temperatures over the period 1884-1983 reconstructed from oxygen isotope ratios of a bivalve mollusk shell (*Arctica islandica*, southern North Sea). Palaeogeogr. Palaeoclimatol. Palaeoecol. 212, 215–232. https://doi.org/10.1016/j.palaeo.2004.05.024.

Schöne, B.R., Houk, S.D., Castro, A.D.F., Fiebig, J., Oschmann, W., Kröncke, I., Dreyer, W., Gosselck, F., 2005a. Daily growth rates in shells of Arctica islandica: assessing sub-seasonal environmental controls on a long-lived bivalve mollusk. PALAIOS 20, 78–92. https://doi.org/10.2307/3515826.

Schöne, B.R., Pfeiffer, M., Pohlmann, T., Siegismund, F., 2005b. A seasonally resolved bottom-water temperature record for the period ad 1866-2002 based on shells of *Arctica islandica* (Mollusca, North Sea). Int. J. Climatol. 25, 947–962. https://doi.org/10.1002/joc.1174.

Scourse, J., Richardson, C., Forsythe, G., Harris, I., Heinemeier, J., Fraser, N., Briffa, K., Jones, P., 2006. First cross-matched floating chronology from the marine fossil record: data from growth lines of the long-lived bivalve mollusc *Arctica islandica*. The Holocene 16, 967–974. https://doi.org/10.1177/0959683606hl987rp.

Shennan, I., Lambeck, K., Flather, R., Horton, B., Mcarthur, J., Innes, J., Lloyd, J., Rutherford, M., Wingfield, R., 2000. Modelling western North Sea palaeogeographies and tidal changes during the Holocene. Geol. Soc. Lond., Spec. Publ. 166, 299–319. https://doi.org/10.1144/gsl.sp.2000.166.01.15.

Smith, D.E., Harrison, S., Firth, C.R., Jordan, J.T., 2011. The early Holocene Sea level rise. Quat. Sci. Rev. 30, 1846–1860. https://doi.org/10.1016/j.quascirev.2011.04.019.

Sturt, F., Garrow, D., Bradley, S., 2013. New models of north west European Holocene palaeogeography and inundation. J. Archaeol. Sci. 40, 3963–3976. https://doi.org/10.1016/j.jas.2013.05.023.

Thompson, I., Jones, D.S., Dreibelbis, D., 1980. Annual internal growth banding and life history of the ocean quahog *Arctica islandica* (Mollusca: Bivalvia). Mar. Biol. 57, 25–34. https://doi.org/10.1007/BF00420964.

Tobin, T.S., Schauer, A.J., Lewarch, E., 2011. Alteration of micromilled carbonate $\delta^{18}O$ during Kiel Device analysis. Rapid Communications in Mass Spectrometry 25, 2149–2152. https://doi.org/10.1002/rcm.5093.

Trofimova, T., Milano, S., Andersson, C., Bonitz, F.G.W., Schöne, B.R., 2018. Oxygen isotope composition of *Arctica islandica* aragonite in the context of shell architectural organization- implications for paleoclimate reconstructions. Geochem. Geophys. Geosyst. https://doi.org/10.1002/2017GC007239.

Uehara, K., Scourse, J.D., Horsburgh, K.J., Lambeck, K., Purcell, A.P., 2006. Tidal evolution of the northwest European shelf seas from the Last Glacial Maximum to the present. J. Geophys. Res. Oceans 111. https://doi.org/10.1029/2006jc003531.

von Leesen, G., Beierlein, L., Scarponi, D., Schöne, B.R., Brey, T., 2017. A low seasonality scenario in the Mediterranean Sea during the Calabrian (early Pleistocene) inferred from fossil *Arctica islandica* shells. Palaeogeogr. Palaeoclimatol. Palaeoecol. 485, 706–714. https://doi.org/10.1016/j.palaeo.2017.07.027.

Waite, A.J., Swart, P.K., 2015. The inversion of aragonite to calcite during the sampling of skeletal archives: Implications for proxy interpretation. Rapid Communications in Mass Spectrometry 29, 955–964. https://doi.org/10.1002/rcm.7180.

Ward, S.L., Neill, S.P., Scourse, J.D., Bradley, S.L., Uehara, K., 2016. Sensitivity of palaeotidal models of the northwest European shelf seas to glacial isostatic adjustment since the last Glacial Maximum. Quat. Sci. Rev. 151, 198–211. https://doi.org/10.1016/j.quascirev.2016.08.034.

Ward, S.L., Scourse, J.D., Yokoyama, Y., Neill, S.P., 2020. The challenges of constraining shelf sea tidal models using seabed sediment grain size as a proxy for tidal currents. Cont. Shelf Res. 205, 104165. https://doi.org/10.1016/j.csr.2020.104165.

Weidman, C.R., Jones, G.A., Kyger, 1994. The long-lived mollusc *Arctica islandica*: A new paleoceanographic tool for the reconstruction of bottom temperatures for the continental shelves of the northern North Atlantic Ocean. J. Geophys. Res. 99, 18305–18314. https://doi.org/10.1029/94jc01882.

Witbaard, R., Jansma, E., Sass Klaassen, U., 2003. Copepods link quahog growth to climate. J. Sea Res. 50, 77–83. https://doi.org/10.1016/s1385-1101(03)00040-6.

Yamanashi, J., Takayanagi, H., Isaji, A., Asami, R., Iryu, Y., 2016. Carbon and oxygen isotope records from *Tridacna derasa* shells: toward establishing a reliable proxy for sea surface environments. PLoS One 11, e0157659. https://doi.org/10.1371/journal.pone.0157659.

Zatsepin, V.I., Filatova, Z.A., 1961. The bivalve mollusc *Cyprina islandica* (L.), its geographic distribution and role in the communities of benthic fauna. Trans. Inst. Oceanol. 46, 2–24.

Zweng, M.M., Reagan, J.R., Antonov, J.I., Locarnini, R.A., Mishonov, A.V., Boyer, T.P., Garcia, H.E., Baranova, O.K., Johnson, D.R., Seidov, D., 2013. World ocean atlas 2013, Volume 2: Salinity. In: Levitus, S. (Ed.), NOAA Atlas NESDIS 74. NOAA, Silver Spring.